Journal of Engineering Physics and Thermophysics, Vol. 73, No. 6, 2000

HEAT EXCHANGE AND HYDRODYNAMICS OF TWO-PHASE MEDIA UNDER CONDITIONS OF FORCED MOTION IN POROUS STRUCTURES

Yu. A. Zeigarnik[a] **and V. M. Polyaev**[b*)]

UDC 536.24

Experimental data on the heat transfer and resistance of two-phase media in porous structures are given. Results of calculating the thermal state of a heat exchanger with a porous insert that is cooled by a two-phase flow are presented.

Introduction. Two-phase heat exchange under conditions of forced motion in channels filled with porous structures is attracting increasing attention. In the 1940s–1960s, researchers' efforts were focused on the study of moisture transfer in porous media [1-3]. Subsequently, the experiments and calculational-theoretical investigations extended to the case of forced motion of two-phase media in porous structures. This is primarily due to the introduction and improvement of the systems of evaporation (transpiration) cooling of apparatuses and energy-converting machinery [4]. They are characterized by a high density of the heat fluxes and intense phase transitions. In many cases, the processes that occur in porous structures are accompanied by thermodynamic nonequilibrium of the phases and hydrodynamic instability of the flows. An appreciable role is played by transfer of heat by heat conduction via the skeleton of a porous structure and the intensity of the internal heat exchange in the porous structure. The problem acquires a substantially conjugate character.

Porous Heat Exchangers with Forced Motion of a Two-Phase Heat-Transfer Agent. Figure 1 gives sketches of heat exchangers with porous inserts in which forced motion of the heat-transfer agent is realized. Figure 1a corresponds to the case of volumetric heat release within the thickness of a porous layer, while in the variant of Fig. 1b heat is supplied to the wall and, via the heat-conducting porous skeleton, is transferred from it to the porous-structure volume. If the skeleton is not heat-conducting, it acts as a turbulizer that enhances mixing. It is more convenient to illustrate the features of the processes occurring using a heat exchanger with unilateral heat supply as an example (Fig. 1b); heat exchangers with bilateral heat supply are, naturally, also used.

Either a single-phase liquid or a liquid-vapor mixture with $(\rho w)_f$ that, in the case under study, is conventionally considered to be homogeneous is supplied to the entrance of the heat exchangers. As the heat-transfer agent moves along the channel, heating (the economizer portion of the heat exchanger), evaporation, and sometimes superheating of it are carried out.

For the heat exchanger of Fig. 1a the phase distribution over the height of the porous layer has the character of congruent fronts of equal enthalpy of the liquid-vapor mixture. Here the process of evaporation is characterized by static instability of the flow. This is predicted analytically [4, 5] and is observed experimentally [6]. To eliminate it, it is necessary to increase the hydraulic resistance (i.e., to decrease the permeability) of the economizer portion.

A somewhat more complex picture of the phase distribution occurs in the heat exchanger of Fig. 1b. In it, the heat that is supplied from the heating wall is transported into the channel through the skeleton of the

*) Deceased.

[a]Institute of High Temperatures, Russian Academy of Sciences, Moscow, Russia; email: zeigar@oivtran.iitp.ru; [b]N. E. Bauman Moscow State Technical University, Moscow, Russia. Translated from Inzhenerno-Fizicheskii Zhurnal, Vol. 73, No. 6, pp. 1125-1134, November–December, 2000. Original article submitted June 29, 1999.

1062-0125/00/7305-1093$25.00

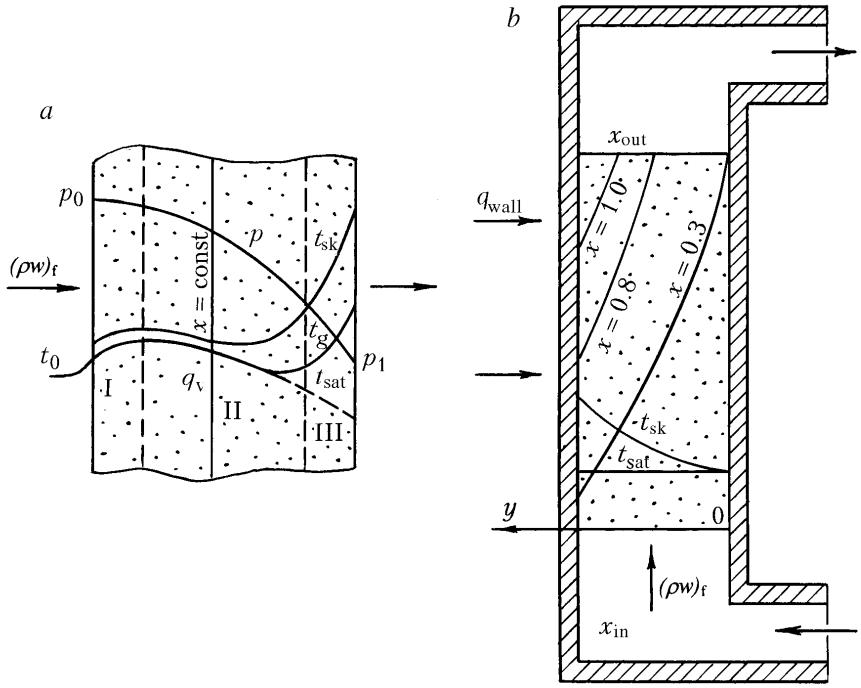

Fig. 1. Sketches of heat exchangers with a porous insert: a) with volumetric heat release [I) liquid phase; II) liquid-vapor mixture; III) superheated vapor]; b) with a heating wall.

porous structure. More heat is removed in the zone adjacent to the heating wall; the skeleton temperature t_{sk}, which approaches t_{sat} with distance from the heating wall, is also higher. The distribution of the parameters of the heat-transfer agent over the channel height y also changes because of the nonuniformity of the heat absorption over the channel cross section. The local mass velocity increases with decrease in y, whereas the vapor quality x, conversely, decreases.

Experimental data on the structure of a two-phase flow obtained with n-pentane for $p \cong 0.1$ MPa, $(w)_f$ = 0.03–0.16 cm/sec, and bilateral uniform side supply of heat with q_{wall} = 2–10 kW/m^2 are given in [7]. The porous insert was a column of bronze spheres 140–160 μm in diameter. The boundaries of the zones of heating, phase transition, and superheating of the vapor were identified according to the data of measurement of the temperature fields. The experiments of [7] confirm to a certain degree the picture shown in Fig. 1b; however the ratio of the dimensions of the zones of heating and evaporation of the liquid turned out to be close to unity in them, whereas under the conditions of [7] the amount of heat required for the phase transition exceeds the amount of heat for heating the liquid to t_{sat} by approximately an order of magnitude. Apparently, the reason has to do with the low velocities of motion of the medium (the reduced vapor velocity did not exceed 0.2 m/sec), which are not sufficient to ensure stable ascending motion of the liquid. Ultimately, it flowed downward, creating a nearly isothermal volume where vapor bubbles formed, i.e., experiments with low values of ρw do not yield representative results.

Experimental Investigation of Heat Transfer and Hydraulic Resistance in the Flow of a Two-Phase Mixture in a Porous Structure. The effect of the regime parameters and the characteristics of the porous structure on the hydraulic resistance and heat transfer is rather complex even for the flow of a single-phase heat-transfer agent [8]. The local coefficient of internal heat transfer α_v or α_s depends on ρw (the Re number = $(\rho w)(\beta/\alpha)/\mu$) and the Pr number of the heat-transfer agent. The size of the elements of the porous structure and its specific characteristics such as the crookedness of the channels are best reflected by the ratio of the inertial β and viscous α coefficients of the generalized Darcy law

$$-(\Delta p/l) = \alpha \frac{(\rho w)\,\mu}{\rho} + \beta \frac{(\rho w)^2}{\rho} = \alpha \frac{(\rho w)\,\mu}{\rho}(1 + \mathrm{Re})\,. \qquad (1)$$

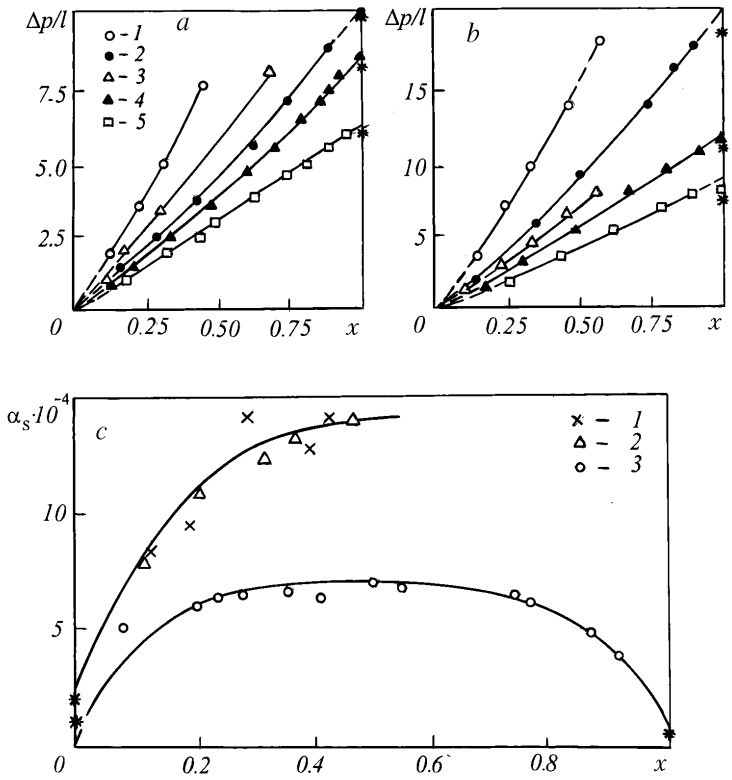

Fig. 2. Experimental data on the hydraulic resistance (a, b) and heat transfer (c) in the flow of a two-phase heat-transfer agent in porous structures [9, 10]: a) specimen No. 11 (d_{part} = 0.30–0.40 mm; Π = 0.41; α = $1.3\cdot10^{10}$ m^{-2}; β = $3.07\cdot10^{5}$ m^{-1}; β/α = 7.69 μm): 1) (ρw) = 27 kg/(m^2·sec); p = 0.59 MPa; 2) 17; 0.59; 3) 13; 0.20; 4) 13; 0.40; 5) 13; 0.59; b) specimen No. 13 (d_{part} = 0.16–0.20 mm; Π = 0.31; α = $3.22\cdot10^{10}$ m^{-2}; β = $2.1\cdot10^{5}$ m^{-1}; β/α = 6.52 μm): 1) 22; 0.59; 2) 15.5; 0.59; 3) 10; 0.30; 4) 10; 0.40; 5) 10; 0.59; c) specimen No. 29 (d_{part} = 0.40–0.63 mm, d_{wire} = 0.51 mm): 1) $(\rho w)_f$ = 31 kg/(m^2·sec), p = 0.4 MPa; 2) 31; 0.6; 3) 21; 0.4; *, calculated values for filtration of water and saturated vapor according to [10]. $\Delta p/l$, MPa/m; α_s, W/(m^2·K).

The two coefficients are taken from experiments.

The indicated parameters also retain their governing effect on heat transfer in the case of a two-phase heat-transfer agent. However, a number of other factors are added to them; among these factors we should place emphasis above all else on the vapor quality x (for small x, the saturation $(1 - \varphi)$ of the porous structure with the liquid phase) and the flow regime of the two-phase flow. The latter factor is of great significance for two-phase flows.

The experimental data on the coefficients of resistance and the internal heat transfer of two-phase flows in a porous structure are sparce. The results of experiments conducted at the Institute of High Temperatures of the Russian Academy of Sciences [9, 10] can be classified among the most systematic data.

Experiments on determining the hydraulic characteristics of two-phase flows were conducted with a water-steam mixture on a direct-flow setup [9]. The flow rate of the heat-transfer agent was provided by a piston pump. To smooth out flow-rate pulsations a damper was installed at the exit of the pump. A water-steam mixture of the required vapor fraction was prepared in a preswitched-on direct-feed evaporator. A pressure drop approximately thrice the resistance of the channel from the entrance of the evaporator to the outlet pipe was created on a valve installed in front of the evaporator. This improved substantially the hydraulic stability of the experimental circuit.

A porous specimen manufactured in the shape of a hollow cylinder was the main element of the working portion. In two cross sections of the specimen spaced 10 mm apart, there were pressure taps. At the entrance to the working portion we installed a mixing system that was expected to ensure a uniform distribution of the phases over the cross section of the flow at the entrance to the test piece.

Specimens made of sintered bronze spheres 160 to 630 μm in diameter with a porosity of 0.28 to 0.44 and a specimen of a highly porous cellular copper material with a porosity of 0.87 were tested. The experiments were conducted under adiabatic conditions in the range of variation of x from 0 to 1, of $(\rho w)_f$ from 10 to 45 kg/(m^2·sec), and of p from 0.2 to 0.6 MPa. Some results are presented in Fig. 2a and b.

A very important component of generalization of experimental data is the development of a physical model of flow that fits reality, i.e., determination of the most probable regime of flow. The qualitative analysis performed and quantitative evaluations showed that at low and moderate pressures even for very small vapor fractions in the pore channel a regime of separate flow of the liquid and vapor phases is, apparently, formed (an analog of the dispersed-annular regime of flow in tubes), when the liquid can exist in the form of a rather thin film on the walls of the channels (pores) and in the form of droplets in the "core" of the flow. Under these conditions, attempts to find the effective ("homogeneous") density and viscosity of the two-phase flow, using which one could describe the obtained experimental data by the Darcy equation (of the type of Eq. (1)), are physically unjustified. Use of the effective density and viscosity, as is done, in particular, in [5, 11], is convenient in terms of calculations but involves errors in the results, especially at low and moderate pressures.

In the general case, the pressure drop in the flow of a two-phase mixture is composed of the pressure loss to friction, the expenditure of pressure on accelerating the phases (vapor, droplets, and film), and the pressure loss in local resistances (contractions, expansions, and rotations of the pores) and on overcoming the hydrostatic head and the capillary forces. Evaluations showed that, under the conditions of the experiments conducted, the pressure loss on overcoming the hydrostatic head can be disregarded, as can the contribution of capillary effects.

The magnitude of the pressure loss on acceleration of the droplets by the vapor core depends on what fraction of the liquid film is removed in droplet form to the vapor core and on the ratio of the droplet and vapor velocities. This loss was evaluated according the procedure of [12]. Because of the small thickness of the liquid film, which is associated with the small cross section of the pore channel, the intensity of wave formation and the removal of droplets are low. The small length of flight of the droplets, because of the crookedness of the pores, causes the low velocity that is acquired by the droplets stripped from the film. Therefore even for an obviously overestimated fraction of liquid removal the pressure loss on acceleration of the droplets in the porous structures investigated does not exceed 2-3% of the total pressure drop.

Calculations also showed that the pressure loss on acceleration of the flow that is associated with the change in the density of the liquid-vapor mixture because of the decrease in the pressure along the length of the porous structure amounts to fractions of a percent of the total pressure drop.

Thus, under the conditions of the experiments conducted, a major contribution to the pressure drop on the test pieces is made by the friction of the liquid film against the pore channels and by the pressure loss that is associated with the flow of the liquid film and the vapor core through local resistances (contractions, expansions, and bends of the pore channel).

Processing of the entire array of experimental data showed the expediency of using for determination of $\Delta p/l$ a computational procedure that is similar to the procedure proposed by Martinelli and Lockhart for the frictional resistance of an adiabatic two-phase mixture in tubes [13], i.e., exactly for the case of separate flow of the phases:

$$(\Delta p/l)_{two} = (\Delta p/l)_{liq}\, \Phi_{liq}^2 \tag{2}$$

or

$$(\Delta p/l)_{two} = (\Delta p/l)_{g}\, \Phi_{g}^2 . \tag{3}$$

Here $(\Delta p/l)_{liq}$ and $(\Delta p/l)_g$ are, respectively, the pressure drops for flow of just the liquid phase in the amount contained in the mixture or just the vapor phase through the porous structure. They are calculated from Eq. (1) in which the corresponding mass filtration rates of each phase are used as the mass filtration rate. According to [13], the parameters Φ_{liq} and Φ_g are functions of the Martinelli parameter $X = \sqrt{(\Delta p/l)_{liq}/(\Delta p/l)_g}$.

The relation of the parameter X to Φ_{liq} and Φ_g is prescribed in the form proposed in [14]:

$$\Phi_{liq}^2 = 1 + C/X + 1/X^2 \tag{4}$$

or

$$\Phi_g^2 = 1 + CX + X^2 . \tag{5}$$

As a result of processing the experimental data it is revealed that, for the data array obtained, the coefficient C is a function of $(\rho w)_f$, the physical properties of the liquid (ρ' and μ'), and the hydraulic characteristics of the porous structure (the coefficients α and β):

$$C = 4\left(\frac{\beta/\alpha}{(\rho w)_f}\frac{\rho'}{\mu'}\right)^{0.4} . \tag{6}$$

The root-mean-square deviation of the results of calculating $(\Delta p/l)$ by formulas (2)-(6) from the experimental values amounts to 12%.

Processing of the experimental results based on a homogeneous flow model failed. The calculated values of $(\Delta p/l)$ throughout the entire range of x, except narrow regions near $x = 0$ and 1.0, exceeded noticeably the experimental values since the homogeneous model overestimates substantially the actual velocity of the liquid phase.

The heat-transfer coefficient was investigated on the same experimental setup as the hydraulic resistance. The working portion was a 35 × 12 mm channel of rectangular cross section in which an electrically heated cylinder – a single wire made of platinum or stainless steel with a diameter d_{wire} = 0.15 or 0.5 mm and a length of 22 mm – was installed transversely to the flow. The channel was filled with hollow zirconium dioxide particles of nearly spherical shape and 0.14 or 0.51 mm diameter, depending on d_{wire}. The height of the charge was about 15 mm. The structure of the flow at the entrance to the charge was formed by a convergent channel and grids with 0.56-mm cells installed behind it. In order to tap pressure, holes were drilled in the skeleton in the cross section where the wire was positioned. In the same cross section, a Chromel–Alumel thermocouple was placed. The wire was heated by a direct electric current from a power supply that operated in the mode of current stabilization. The average temperature of the wire was found using its measured electrical resistance from the temperature dependence of the resistance determined previously. The saturation temperature was determined from the measured pressure. The details of the procedure are described in [15]. The procedure provides the required uniformity of the heat-flux density on the heat-transfer element and acceptable accuracy of its measurement and accuracy and determinacy of measuring the temperature of the heating surface.

Data on the heat-transfer coefficients were obtained in the range of the parameters x = 0–1.0, $(\rho w)_f$ = 10–35 kg/(m^2·sec), p = 0.2–0.6 MPa, $q_s = 0–1.6\cdot10^6$ W/m^2; the porosity was 0.46 for a charge of particles with d_{part} = 0.125–0.160 mm and Π = 0.36 for a charge of particles with d_{part} = 0.40–0.63 mm. Characteristic results of measuring the heat transfer are shown in Fig. 2c.

The effect of x on the heat-transfer coefficient α_s is nonmonotonic: in the range of x from 0 to approximately 0.5, an increase in α_s is observed, whereas the heat-transfer coefficient decreases with further increase in x. An increase in ρw and a decrease in d_{part} cause α_s to increase.

For x = 0, the experimental data obtained agree well with results of investigations of the heat transfer in filtration of a single-phase liquid (they are marked with an asterisk in Fig. 2). For $x \to 1$, the experiments

yielded values of α_s distinctly higher than those in filtration of a saturated vapor, which is attributable to the presence of droplets of nonequilibrium moisture in the flow of the vapor generated by the preswitched-on vapor generator.

The behavior of the curves in Fig. 2c can be explained qualitatively as follows. In the case of flow of a single-phase liquid ($x < 0$), convective transfer of heat from the wire surface occurs. Passage to a two-phase mixture yields a significant increase in α_s. For small values of x (several percent), this is apparently caused by passage to heat transfer with a change in the state of aggregation. A further increase in x leads to replacement of the flow regime of the mixture: the liquid phase begins to move in the form of a thin film over the pore walls. Here, the heat transfer occurs by evaporation from the film surface; it is characterized by high intensity and is limited by the thermal resistance of the film. An increase in x leads to thinning of the film and an increase in α_s.

For large x, the film comes off part of the wire surface, which is associated to some degree with an increase in the tangential stresses at the interphase boundary. On the remaining part of the surface, near sites of contact of the particles with the wire, the film is held by surface tension forces. In this situation, we have a certain integral value of α_s. It is reasonable to suppose that, in heating the entire mass of the porous body, the mechanism of heat transfer will be qualitatively similar to the mechanism described above.

The surface heat-transfer coefficients α_s can be converted to volumetric ones α_v using the formula

$$\alpha_v = 6\alpha_s (1 - \Pi)/d_{part} . \tag{7}$$

At present, there are no universally adopted methods of generalization of heat transfer for two-phase flows in channels. Under these conditions, one often seeks to describe experimental data by relating them to heat-transfer coefficients that are calculated from formulas of forced convection of a single-phase heat-transfer agent under the same geometric conditions [16]. This technique was also used in generalization of experimental results obtained at the Institute of High Temperatures of the Russian Academy of Sciences, and data on heat transfer to a single-phase heat-transfer agent were obtained with the same specimens with which heat transfer to a water-steam mixture was studied. Ultimately, we have the formula

$$\alpha/\alpha_{liq} = 1 + Kx\sqrt{\left(\frac{1-x}{x}\right)}, \tag{8}$$

where

$$K = 810\sqrt{\left((\rho w)_f \frac{\nu'}{\sigma}\right)}. \tag{9}$$

The combination under the square-root symbol in relation (9) is obtained from considerations of dimensionality; the parameters involved in it are selected based on general ideas of the mechanism of the process since $(\rho w)_f$, σ, and ν' each have an effect on the thickness and flow of the film. The root-mean-square deviation of values of α_s that are calculated from (9) and (10) from the experimental data does not exceed 20%. Clearly the experimental results presented need to be complemented.

The hydraulic resistance of a porous matrix in a boiling two-phase flow was investigated experimentally in [11] under conditions of heat transfer substantially less intense than in [10]. The experiments were conducted with forced filtration of a water-steam flow in a charge of inductively heated steel spheres 0.59 to 4.76 mm in diameter for $(\rho\omega)_f$ = 0.14–5.05 kg/(m^2·sec) and q_v = 1.44–44 W/cm^3.

According to [11], the hydraulic resistance increases with $(\rho w)_f$ and x_{mixt}, which is in agreement with experimental data of the Institute of High Temperatures of the Russian Academy of Sciences. In our opinion, the obtained absolute values of the volumetric vapor fraction φ and the character of its change as a function of x indicate that separate flow of the phases rather than a homogeneous structure of the flow existed in the experiments.

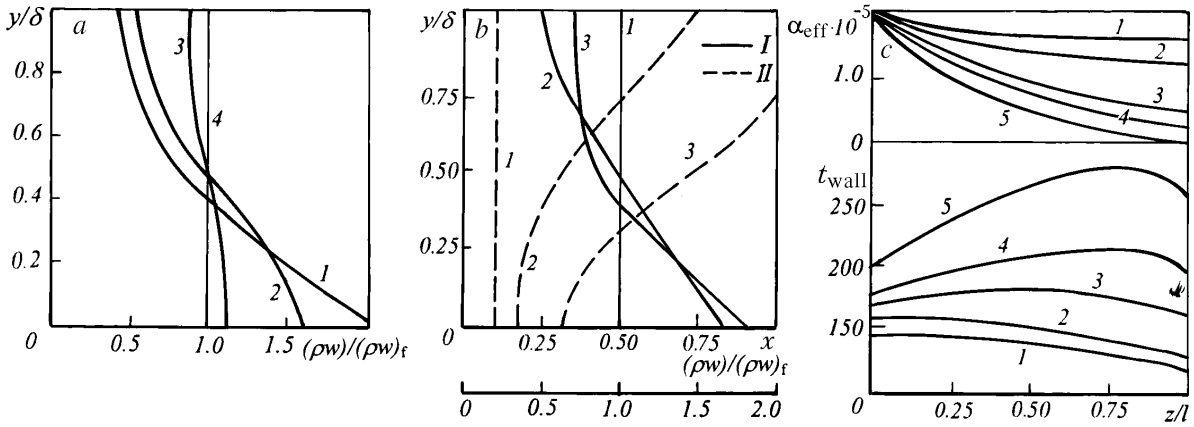

Fig. 3. Thermal state of a heat exchanger with a porous insert: a) distribution of the relative mass velocity $(\rho w/(\rho w)_f$ over the height of the porous matrix at distance z/l = 0.4 from the inlet to the porous insert for different vapor qualities at the entrance to the insert; d_{part} = 300–400 μm; δ = 5 mm; l = 50 mm; Π = 0.4; λ_{part} = 400 W/(m·K); q_{wall} = 1 MW/m^2; $(\rho w)_f$ = 10 kg/(m^2·sec); p_{out} = 0.1 MPa: 1) x_{in} = 0.01; 2) 0.1; 3) 0.5; 4) 0.75; b) distribution of the relative mass velocity $(\rho w)/(\rho w)_f$ (*I*) and the vapor quality x (*II*) over the height of the porous insert at different distances z/l from the inlet to the insert (d_{part} = 300–400 μm; δ = 5 mm; l = 50 mm; Π = 0.4; λ_{part} = 400 W/(m·K); q_{wall} = 1 MW/m^2; $(\rho w)_f$ = 10 kg/(m^2·sec); x_{in} = 0.1; p_{out} = 0.1 MPa): 1) z/l = 0; 2) 0.4; 3) 1.0; c) change in the effective heat-transfer coefficient α_{eff} and the temperature of the heating wall t_{wall} along the channel for different values of the heat-flux density (d_{part} = 300–400 μm; δ = 5 mm; l = 50 mm; Π = 0.4; λ_{part} = 400 W/(m·K); $(\rho w)_f$ = 10 kg/(m^2·sec); x_{in} = 0.1; ρ_{out} = 0.1 MPa): 1) q_{wall} = 0.5 MW/m^2; 2) 1.0; 3) 2.0; 4) 3.0; 5) 5.0. α_{eff}, W/(m^2·K); t_{wall}, ^{o}C.

Thermal State of a Porous Heat Exchanger. It has already been noted that the distribution of the parameters of a two-phase flow through the volume of a porous insert is distinguished by high nonuniformity. It is affected by the regime parameters and the geometric and thermophysical characteristics of the porous insert. Ultimately, in order to determine and optimize the thermal state of a heat exchanger, one has to solve a conjugate thermohydraulic problem for the heat-transfer agent and the porous skeleton.

At the Institute of High Temperatures of the Russian Academy of Sciences, a computational program was developed and a parametric investigation of heat exchangers with porous inserts was performed. Figure 3 illustrates the special properties of the phenomena; they were considered in greater detail in [17].

Figure 3a shows the distribution of the relative mass velocity $(\rho w)/(\rho w)_f$ over the height of the porous matrix for different vapor qualities at the entrance to the heat exchanger. Here and subsequently the basic regime parameters and the characteristics of the heat exchanger are given in the caption. Strong deformation of the profile of ρw is seen. It is associated with the fact that, near the heating wall, vapor formation is more intense; the vapor quality x also increases faster. This increases the hydraulic resistance to the flow in this zone and decreases the fraction of the flow of the heat-transfer agent near the wall. The decrease in ρw causes x to increase further. As the entrance vapor quality x_{in} increases, the nonuniformity of the distribution of ρw over the channel height decreases, and it almost disappears at x_{in} = 0.75.

It is seen from Fig. 3b that, when the heat-flux density on the wall q_{wall} is rather high, $x > 1$ near the heating wall at the exit from the heat exchanger, i.e., the elements of the porous structure near the wall are completely dried. At the same time, the moisture content of the flow $(1 - x)$ remains rather high at a distance from the wall. If the increased mass velocity in this region is taken into account, it becomes clear that, in spite

of overheating of the skeleton relative to the saturation temperature t_{sat}, the degree of drying of the flow is low on the whole.

Figure 3c illustrates the change in the effective heat-transfer coefficient $x_{eff} = q_{wall}/(t_{wall} - t_{sat})$ and in the temperature of the heating wall t_{wall} along the channel. It is seen that α_{eff} decreases along the channel, which above all is associated with an increase in the mean vapor fraction and a decrease in ρw near the wall. The coefficient α_s decreases with increase in q_{wall}, which is attributable to diminished use of the height of the porous insert – the skeleton is overheated to a larger depth. The decrease in t_{wall} along the channel for relatively low q_{wall} (curves 1 and 2) is caused by a decrease in the pressure p_{sat}. For high values of q_{wall}, the wall temperature increases substantially because of drying of the part of the skeleton adjacent to the heating surface.

The quantity t_{wall} is affected strongly by the height of the porous insert. When the channel height is small, it is difficult to provide a substantial flow rate of the coolant. When the height is large, the matrix layers and coolant jets at a distance from the heating wall are used inefficiently.

An increase in ρw intensifies heat transfer; however, this does not necessarily cause t_{wall} to decrease because of an increase in the hydraulic resistance.

The effect of the thermal conductivity of the skeleton is in many respects similar to the effect of the height of the insert. A decrease in λ_{part} causes an increase in the fraction of heat transferred near the heating wall. If an insert of height δ = 5 mm is manufactured of bronze particles rather than copper ones, t_{wall}, even for q_{wall} = 1 MW/m^2, will increase along its entire length, attaining 300^{o}C already at the center of a 50-mm-long porous insert (as earlier, the output pressure was taken to be equal to 0.1 MPa).

The effect of the porosity Π on t_{wall} is ambiguous. As Π increases, the heat-transfer coefficient and the thermal conductivity of the skeleton decrease, but the pressure drop along the channel also decreases.

Conclusion. Filling the volume of the channel of a heat exchanger with a two-phase heat-transfer agent with a porous material makes it possible, in many cases, to substantially intensify heat transfer from the channel walls. The characteristics of the inserts and the parameters of the heat-transfer agent can be selected only by means of detailed variant calculations. Individual parameters have a strong effect on each other. Therefore the selection of the characteristics of the heat exchanger depends largely on the objectives of the problem solved (a decrease in the temperature drop between the heating wall and the coolant, stabilization of the wall temperature, etc.). An additional factor here can be provision of the required flow rate of the heat-transfer agent or limitation of the pressure drop on the channel.

An increase in the heating-surface temperature that occurs for one reason or another is not of a crisis nature – the temperature increases gradually and fails to attain values that are typical of two-phase flows in channels without porous inserts when the critical density of the heat flux is exceeded.

NOTATION

d, diameter; l, length; p, pressure; q, heat-flux density; t, temperature; w, velocity; x, vapor quality; y, transverse coordinate (see Fig. 1b); z, longitudinal coordinate; α, heat-transfer coefficient, viscous coefficient of friction; β, inertial coefficient of friction; φ, volumetric vapor fraction; σ, surface tension; λ, thermal conductivity; μ, dynamic coefficient of viscosity; Π, porosity; ρ, density; ν', kinematic coefficient of viscosity; ρw, mass velocity; Pr, Prandtl number; Re, Reynolds number; Φ and X, Martinelli parameters. Subscripts: two, two-phase; sk, skeleton; wire, wire; mixt, mixture; wall, wall; part, particle; f, filtration; g, gas (vapor) phase; liq, liquid phase; s, surface; sat, saturation state; v, volumetric; primed symbols, parameters of the liquid phase on the saturation line.

REFERENCES

1. A. V. Luikov and Yu. A. Mikhailov, *Theory of Heat and Mass Transfer* [in Russian], Moscow (1962).
2. S. Whitaker, *Adv. Heat Transfer*, **13**, 119-203 (1977).
3. O. G. Martynenko and N. V. Pavlyukevich, *Inzh.-Fiz. Zh.*, **71**, No. 1, 5-18 (1998).

4. V. M. Polyaev, V. A. Maiorov, and L. L. Vasil'ev, *Hydrodynamics and Heat Exchange in Porous Elements of Aircraft Structures* [in Russian], Moscow (1988).
5. L. L. Vasil'ev and V. A. Maiorov, *Int. J. Heat Mass Transfer*, **22**, No. 2, 301-307 (1979).
6. V. M. Polyaev and A. V. Sukhov, *Teplofiz. Vys. Temp.*, No. 7, 1037-1039 (1969).
7. O. Rahli, F. Topin, L. Tadrist, and J. Pantaloni, *Int. J. Heat Mass Transfer*, **39**, No. 18, 3959-3975 (1996).
8. Yu. A. Zeigarnik and V. M. Polyaev, *Teploénergetika*, No. 1, 62-70 (1996).
9. Yu. A. Zeigarnik and I. V. Kalmykov, *Teplofiz. Vys. Temp.*, **23**, No. 5, 934-940 (1985).
10. Yu. A. Zeigarnik and I. V. Kalmykov (Kalmikov), *Exp. Heat Transfer*, **4**, 59-69 (1991).
11. A. S. Naik and V. K. Dhir, *Int. J. Heat Mass Transfer*, **25**, No. 4, 541-552 (1982).
12. Yu. A. Zeigarnik and V. D. Litvinov, *Boiling of Alkali Metals in Channels* [in Russian], Moscow (1983).
13. R. W. Lockhart and R. G. Martinelli, *Chem. Eng. Progr.*, **45**, No. 1, 39-48 (1949).
14. D. Chisholm and L. A. Sutherland, *Proc. Inst. Mech. Engrs.*, **184**, Pt. 3c, 24-32 (1962).
15. I. V. Kalmykov, *Heat Exchange and Hydrodynamics in the Motion of a Water-Steam Flow in Porous Media*, Candidate's Dissertation in Technical Sciences, Moscow (1987).
16. V. E. Shrock and L. M. Grossman, *Nucl. Sci. Eng.*, **12**, No. 4, 474-481 (1962).
17. Yu. A. Zeigarnik and I. V. Kalmykov (Kalmikov), in: *Proc. Int. Symp. on Phase Change Heat Transfer*, Chongquin, China, May 20-23 (1988), pp. 465-469.